NCREE NEWSLETTER

March 2024 VOL. 19 NO. 1

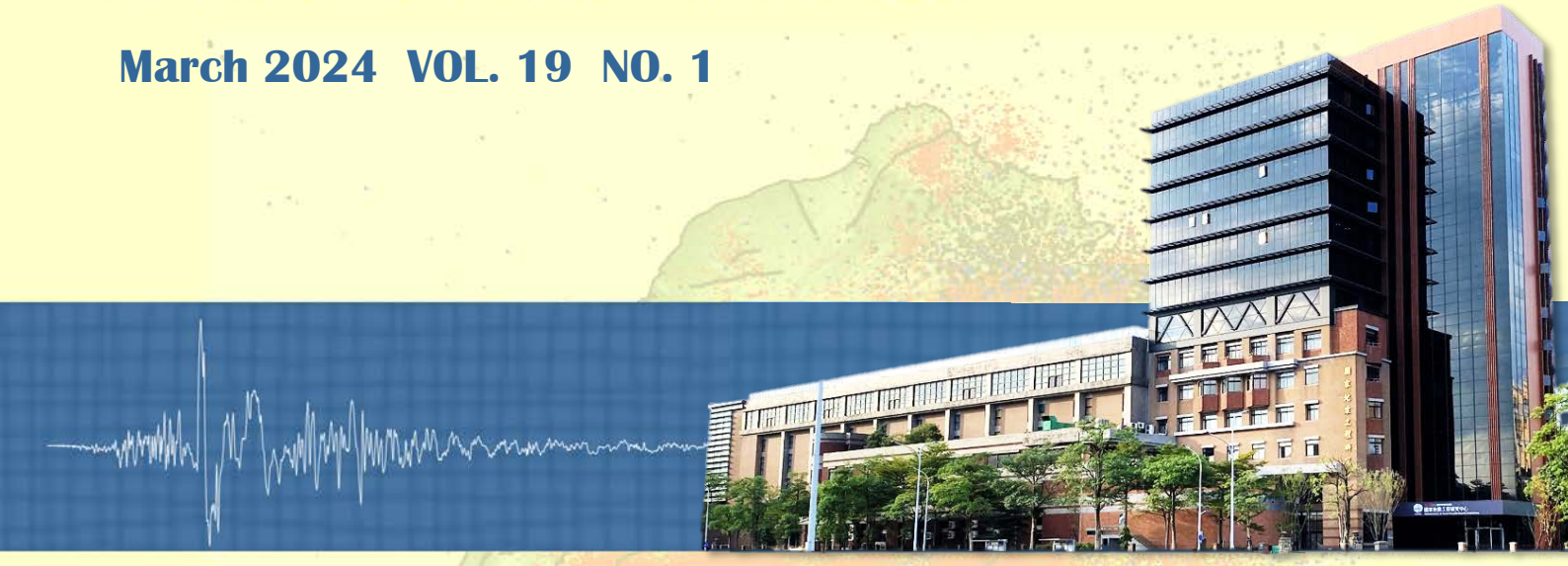

CONTENTS

- Recommendations on Seismic Performance Assessment Criteria for Reinforced Concrete Beam-Column Joints
- Development of a Steel Frame Reinforcement Construction Method for Brick Wall Openings
- Simplified Nonlinear Modeling for Estimating the Seismic Response of Buildings
- Revised Recommendations of CNS 12618 Annex A for Straight Beam Ultrasonic-Testing Probe Specifications for Melting Edge Measurement
- Seismic Rapid Evaluation Using AI Technology
- Seismic Evaluation of Steel Buildings (TEASPA-S)
- Validation of the Numerical Model of the Extended NCREE Building Using Measured Seismic Responses
- Analysis of Truss-Confined Buckling-Restrained Braces
- Nonlinear Dynamic Analysis for Seismic Retrofitting Applications
- Seismic Study on Shear-type Seismic Stud Columns
- Confinement Reinforcement of High-Strength Reinforced Concrete Tied Columns under High Axial Loads
- Soft Retrofit - An Interior Seismic Retrofitting Technique for RC Buildings Using Steel Elements
- Robotic Welding Technology for Continuity Plate Welding Within Steel Built-up Box Columns
- Workshop of Needs and Aspirations for Disaster Prevention and Rescue Needs with Artificial Intelligence Technology
- NCREE Exhibits at CES 2024 and Signs MOU with ActiBooty Inc.
- NCREE Signs MOU with the Earthquake Research Center of Thailand (EARTH)
- Memorandum of Understanding between SESTEC and NCREE

National Center for Research on Earthquake Engineering

Recommendations on Seismic Performance Assessment Criteria for Reinforced Concrete Beam-Column Joints

Kai-Ning Chi, Assistant Researcher, NCREE
Ker-Chun Lin, Research Fellow, NCREE
Sheng-Jhih Jhuang, Assistant Researcher, NCREE

To confirm the seismic performance of reinforced concrete (RC) beam-column joints and to further understand the influence of design parameters on their seismic behavior, such as "the anchorage length of longitudinal bars," "demand and capacity of shear force ratio," "connected types of steel bars" and "failure modes" within the joint area, the ACI 374.1-05 seismic performance evaluation criterion will be used for analysis, and the inspection standards based on strength, stiffness, and energy assessments, will be appropriately adjusted to account for the influence of the aforementioned parameters on the seismic performance of beam-column joints. The author's research team has conducted over 40 sets of beam-column joint tests. Considering that joint specimens satisfying seismic design requirements typically exhibit maximum strength at a beam deformation of 4% or greater, the team observed that the strength decay of the joint is approximately 10% in repeated loops of 4% drift ratio. In addition, according to the special provisions of the Seismic Provisions for Structural Steel Buildings (AISC 341-10), the seismic performance evaluation of steel beam-column joints is based on a 4% drift ratio. To ensure that the joints of reinforced concrete and steel have the same deformation capacities under the action of earthquakes, this study recommends using the test results corresponding to a 4% drift ratio, which generally yields a stable strength response, for evaluating the seismic performance of RC beam-column joints.

A total of 31 sets of external beam-column joint specimens were used in this study. All specimens adhered to the requirements stipulated for strong columns and weak beams in concrete structure design specifications. Key research parameters, including the anchorage length of beam bars, demand and capacity of shear force ratio, types of steel bar connections, and net spacing of steel bars in the joint area, are summarized in the table.

Assessment of Seismic Performance

Upon evaluating the seismic performance of beam-column joints based on the ACI 374.1-05 criterion and the method proposed in this study, it was observed that, barring specimens whose anchorage lengths of beam bars did not comply with design specifications, and hence failed to meet the strength and stiffness criteria outlined in the evaluation methods, all other specimens were deemed satisfactory. Numerical comparison revealed that the ACI 374.1 criteria check values for stiffness and energy are less effective in assessing performance, whereas the evaluation standards recommended in this study can more accurately assess the seismic performance of joints. It is recommended to employ this evaluation method to assess the seismic performance of beam-column joints. The evaluation criteria rules proposed in this study are as follows:

Strength: During cyclic loading testing, the strength at drift ratios within ±4% of the first loop should not be less than 0.9 times the maximum strength.

Energy: During cyclic loading testing, the energy dissipation area at drift ratios within ±4% of the second loop should not be less than 0.8 times the area of the first loop.

Stiffness: During cyclic loading testing, the secant stiffness within a ±0.40% drift ratio range of the second loop should not be less than 0.6 times the equivalent stiffness of the first loop.

Beam-Column Joint Specimens	f_c' (MPa)	f_{ce}' / f_{ge}' (MPa)	Column b	Column h (mm)	Beam b	Beam h (mm)	Main bars	s (d_b)	l_{ext}/d_b	$V_{p,n}/V_n$
JT6_TB528_L	42	46.8	650	650	400	700	T 6-#8 B 6-#8	2.2	21.1	0.59
	420	445	650		700			2.2	21.1	
JT6_T309B216_L_1	42	50.0	650	650	400	700	T 6-#8 B 6-#8	2.2	12.4	0.61
	420	445	650		700			2.2	8.6	
JT6_T309B216_L_2	42	50.2	650	650	400	700	T 6-#8 B 6-#8	2.2	12.4	0.61
	420	465	650		700			2.2	8.6	
JT6_T450B380_L	42	53.8	650	650	400	700	T 6-#8 B 6-#8	2.2	18.0	0.61
	420	465	650		700			2.2	15.2	
JT6_TB309_L	42	50.0	650	650	400	700	T 6-#8 B 6-#8	2.2	12.4	0.61
	420	465	650		700			2.2	12.4	
JT8_TB358_H	42	41.5	550	600	400	600	T 8-#8 B 8-#8	2	14.3	1.01
	420	456	600		600			2	14.3	
JT8_TB358_M	42	47.8	650	600	400	600	T 8-#8 B 8-#8	2	14.3	0.85
	420	456	600		600			2	14.3	
JT8_TB358_L	42	44.6	750	600	400	600	T 8-#8 B 8-#8	2	14.3	0.74
	420	456	600		600			2	14.3	
JT8_TB323_H	42	42.6	550	600	400	600	T 8-#8 B 8-#8	2	12.9	1.01
	420	456	600		600			2	12.9	
JT8_TB323_M	42	47.5	650	600	400	600	T 8-#8 B 8-#8	2	12.9	0.85
	420	456	600		600			2	12.9	
JT8_TB440_H	42	38.8	550	600	400	600	T 8-#8 B 8-#8	2	17.9	1.01
	420	456	600		600			2	17.6	
JT6/4_T500B400_M	42	49.7	600	600	400	600	T 3-#8 T 3-#10 B 2-#8 B 2-#10	2	19.7 15.5 15.7 12.4	0.76
	420	487/494	600		600			2		
JT6/4_T500B400_L_MS	42	48.3	600	600	400	600	T 6-#8 T 4-#8	2.6	19.7	0.72
	550	613	600		600			2.6	15.5	
JT6/4_TB400_L_MS	42	43.3	600	600	400	600	T 6-#8 T 4-#8	2.6	15.5	0.72
	550	613	600		600			2.6	15.5	
JT6_TB390_L_HS	70	81.2	600	600	400	700	T 6-#8 B 6-#8	2	15.4	0.76
	685	709	600		700			2	15.4	
JT6_TB390_L_HS_HA	70	84.1	600	600	400	700	T 6-#8 B 6-#8	2	15.4	0.76
	685	709	600		700			2	15.4	
JT8_TB390_H_HS	70	93.8	600	600	400	600	T 8-#8 B 8-#8	2	15.4	1.02
	685	709	600		600			2	15.4	
JT8_TB390_H_HS_HA	70	89.8	600	600	400	600	T 8-#8 B 8-#8	2	15.4	1.02
	685	709	600		600			2	15.4	
JT4_TB580_L	28	39.0	600	700	500	650	T 4-#11 B 4-#11	2.35	16.2	0.81
	420	461	700		650			2.35	16.2	
JT4_TB580_L_MS	42	34.1	600	700	500	650	T 4-#11 B 4-#11	2.35	16.2	0.83
	550	568	700		650			2.35	16.2	
JT4_TB580_L_HS	69	32.7	600	700	500	650	T 4-#11 B 4-#11	2.35	16.2	0.81
	690	749	700		650			2.35	16.2	
JT5_TB580_H	28	42.7	600	700	500	650	T 5-#11 B 5-#11	1.5	16.2	1.01
	420	461	700		650			1.5	16.2	
JT5_TB580_H_MS	42	50.1	600	700	500	650	T 5-#11 B 5-#11	1.5	16.2	1.03
	550	568	700		650			1.5	16.2	
JT5_TB580_H_MS_HA	42	45.9	600	700	500	650	T 5-#11 B 5-#11	1.5	16.2	1.03
	550	568	700		650			1.5	16.2	
JT5_TB580_H_HS	69	44.5	600	700	500	650	T 5-#11 B 5-#11	1.5	16.2	1.01
	690	749	700		650			1.5	16.2	
JT5_TB580_H_HS_HA	69	44.1	600	700	500	650	T 5-#11 B 5-#11	1.5	16.2	1.01
	690	749	700		650			1.5	16.2	
JT6_TB580_H	28	78.9	600	700	500	650	T 6-#11 B 6-#11	2.35	16.2	1.23
	420	461	700		650			2.35	16.2	
JT6_TB580_H_MS	42	69.9	600	700	500	650	T 6-#11 B 6-#11	2.35	16.2	1.26
	550	568	700		650			2.35	16.2	
JT6_TB580_H_MS_HA	42	85.6	600	700	500	650	T 6-#11 B 6-#11	2.35	16.2	1.26
	550	568	700		650			2.35	16.2	
JT6_TB580_H_HS	69	86.3	600	700	500	650	T 6-#11 B 6-#11	2.35	16.2	1.23
	690	749	700		650			2.35	16.2	
JT6_TB580_H_HS_HA	69	76.0	600	700	500	650	T 6-#11 B 6-#11	2.35	16.2	1.23
	690	749	700		650			2.35	16.2	

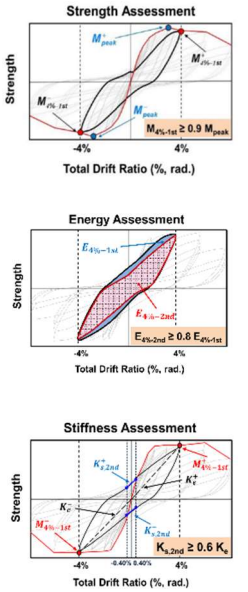

Review and Suggestions

The research results indicate that the RC beam-column joint aligns with the seismic design provisions of the concrete structure design code, satisfying the seismic performance evaluation criteria outlined in ACI 374.1 as well as those recommended in this study. Comparing the ACI 374.1 criterion and the proposed method revealed that the latter can more accurately assess the seismic performance of joints. It is recommended to use this evaluation standard for assessing the seismic performance of RC beam-column joints.

Development of a Steel Frame Reinforcement Construction Method for Brick Wall Openings

Yuan-Tao Weng, Associate Researcher, NCREE
Gee-Jin Yu, Associate Technologist, NCREE
Te-Kuang Chow, Associate Technologist, NCREE

Typical low-rise street houses constructed of reinforced concrete (RC) or reinforced bricks are common in central and southern Taiwan. Based on experience of earthquake disaster surveys over many years, these buildings often have a large number of partition walls perpendicular to the street and parallel to the street for ventilation, lighting, pipes, and ventilation, etc. Due to the demand, there are frequent openings with large areas, which cannot be equipped with complete walls, thus forming a weak surface and weakening the seismic resistance of the building. Earthquakes frequently cause weak ground floor damage along the street direction. The purpose of the reinforcement proposed in this study is to overcome the need for space usability and accommodate the need for wall openings or pipes. It comprehensively considers the structural characteristics of brick walls and user needs and employs a simple method that is low-cost and sufficiently effective. It is expected to be used in on-site construction to increase the willingness of private building owners to carry out seismic reinforcement repairs.

The construction method is based on the basic concept of reinforcing the perimeters of the brick wall openings. The method uses steel components, which are lightweight and easily processed and installed. The steel components are connected using bolts (within the brick wall thickness of 1B) or anchored with chemical anchors during design. Epoxy or non-shrinkage cement is then poured between the brick wall opening and the steel component to enhance shear strength around the opening. The advantages of the proposed method are as follows:

- Minimization of on-site interference.
- Requirement of only steel and epoxy or non-shrinkage cement.
- Cost-effectiveness.
- Feasibility of implementation within the structure, with minimal interference on neighboring buildings.

Features and Precautions

(1) Compliance with lighting and ventilation requirements.

(2) Minimal impact on usable space.

(3) Effective shortening of the construction duration, elimination of template engineering, and reduction of time-related expenses.

(4) Emphasis on anti-seepage construction of the interface of brick wall openings.

Before using this reinforcement construction method, the following two relevant provisions of building brick structure design and construction specifications must be adhered to: (1) The total length of openings in a single wall shall not exceed one-half of the length of the wall; for each floor, the total length of the openings shall not exceed one-third of the total length of the walls on the floor. (2) The distance between the openings or between the edges of the openings and the center line of the intersecting walls or other supports shall be at least twice the wall thickness or greater than 60 cm; however, this does not apply if the openings are reinforced with reinforced concrete or steel frames.

Retrofitting Design Implications

(1) The steel plate should be 4~6 mm thick A36 steel or a steel of equivalent or higher grade. The chemical anchor bolt should be made of ISO 898 5.8 grade galvanized screw or a steel of the same grade. The size should be within M10 specifications. The designer should consider the design requirements and construction conditions, which will be determined after thorough communication with the owner.

(2) For the construction of chemical anchors, product specifications should be established, holes should be thoroughly cleaned after drilling, and pull-out tests should be conducted before construction.

(3) The distance between chemical anchor bolts or bolts used to assemble the open steel frame should not exceed 40 cm, and the distance from the outer edge of the steel plate should be at least 2.5 cm.

(4) When two L-shaped steel plates are welded together, I-type penetration welding should be used. The welding bead length should be a minimum of 100 mm, and the welding bead spacing should not exceed 300 mm.

(5) The reinforced strength must be sufficient to withstand the weight of the opening from both sides upward within an angle of 45 degrees. Non-structural walls should also satisfy this requirement.

A suggested reference diagrams is illustrated in Fig. 1.

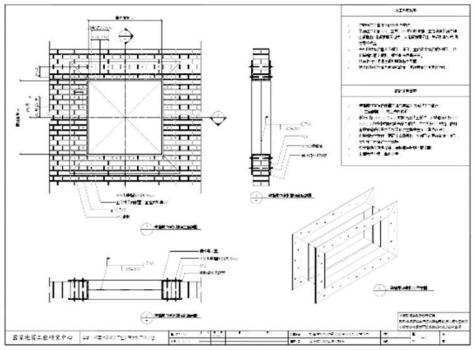

Fig. 1. Schematic diagram of typical street house brick wall opening reinforcement construction method (brick wall thickness below 1B)

Simplified Nonlinear Modeling for Estimating the Seismic Response of Buildings

Jui-Liang Lin, Research Fellow, NCREE
Ming-Chieh Chuang, Associate Researcher, NCREE

Simplified seismic analyses of buildings are typically conducted using either simplified analysis methods or simplified numerical modeling. The advantage of using simplified analysis or modeling lies in the improved efficiency of seismic evaluation, which is a trade-off against the accuracy of the analysis results. With regard to simplified numerical modeling, using modal systems or stick models instead of complete finite element models (FEMs) for building structures is a common approach.

Using simplified numerical modeling is advantageous for identifying critical structural parameters, enabling designers to efficiently grasp structural characteristics. Therefore, simplified numerical modeling is particularly suitable for preliminary design and parametric studies of building structures. Moreover, using simplified numerical modeling facilitates the rapid evaluation of seismic risk in populated cities with numerous buildings. The exploration and application of simplified numerical modeling in earthquake engineering have been comprehensively conducted.

In order to simulate the complex behavior of elastic tall wall-frame buildings, the continuous beam model (Fig. 1(a)) was proposed in the 1960s. The continuous beam model, wherein the mass is continuously distributed along the beam length, consists of two continuous beams connected with each other through axially rigid links (Fig. 1 (a)). One of the two continuous beams is a flexural beam, which deforms in a pure flexural mode. The other continuous beam is a shear beam, which deforms in a pure shear mode. By adjusting the ratio of the shear rigidity of the shear beam to the flexural rigidity of the flexural beam, the continuous beam model can simulate coupled shear-flexure deformation in tall buildings. The continuous beam model has been widely applied to the seismic evaluation of tall buildings.

Inspired by the versatile applications of the continuous beam model (Fig. 1(a)), the authors proposed the generalized building model (GBM), which consists of one shear stick and one flexural stick (Fig. 1(b)). The GBM allows irregular distributions of story mass and story stiffness along the building height. By contrast, the continuous beam model (Fig. 1(a)) simulates buildings with only regular (e.g., uniform, linear, or parabolic) distributions of story mass and story stiffness along the building height. Moreover, because the mass is continuously distributed along the beam length, the continuous beam model is typically suitable only for simulating high-rise buildings. A GBM with discrete (i.e., lumped) masses at floor level is suitable for simulating buildings with any number of stories.

The present study aims to enhance the existing GBM by incorporating inelastic properties, enabling it to serve as a simplified numerical model for estimating the nonlinear seismic response of buildings. The results of this study are expected to provide an alternative method of simplified nonlinear modeling of buildings without restrictions on deformation type, number of stories, or distribution of story mass and stiffness along building heights. The two sticks of each story of the GBM are simulated as beam-column elements with lumped plasticity at their top and bottom. The collective force-deformation relationship of the two sticks of the *r*th story of the GBM is expected to reflect the force-deformation relationship of the *r*th story in the FEM.

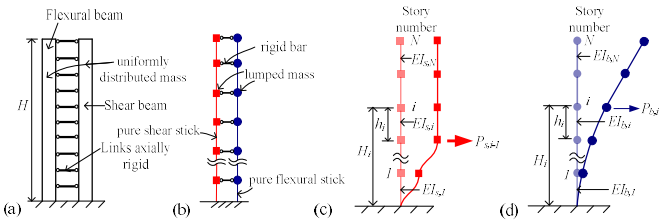

Fig. 1. (a) Continuous beam model; (b) GBM; (c) lateral deformation of a pure shear stick subjected to a concentrated lateral load, $P_{s,i-1}$, at the $(i-1)$th story; and (d) lateral deformation of a pure flexural stick subjected to a concentrated lateral load, $P_{b,i}$, at the ith story.

Numerical Validation

A nine-story steel building, the prototype used in the SAC steel research project for buildings located in Los Angeles, was used in this study. Results of GBM analysis are summarized in Figure 2, which illustrates that the GBM effectively estimated both peak values and phases of seismic responses for the nine-story building. Overall, the GBM proves to be a viable alternative simplified nonlinear model for estimating the seismic response of the nine-story building.

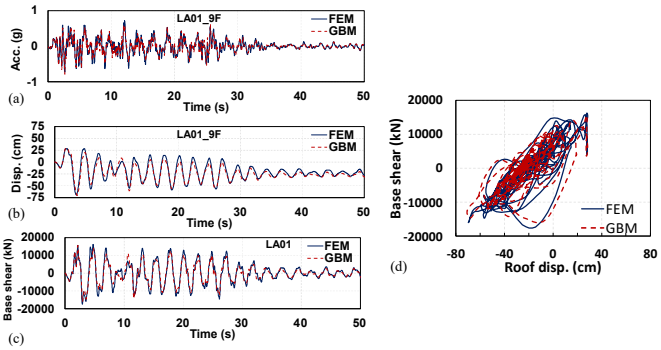

Fig. 2. Histories of (a) roof (9F) acceleration, (b) roof (9F) displacement, (c) base shear, and (d) hysteretic loop of roof displacement versus base shear in response to ground motion LA01.

Revised Recommendations of CNS 12618 Annex A for Straight Beam Ultrasonic-Testing Probe Specifications for Melting Edge Measurement

Ker-Chun Lin, Research Fellow, NCREE

In general, the construction of steel buildings in Taiwan mostly refers to Japanese engineering practices, in which, the column members often utilize built-up box columns composed of four steel plates. However, North American engineering practices in the north American is quite different, in that the columns typically use heavy H-shaped steel as column members within steel buildings. Each box column needs to be installed with internal diaphragms at connections to beams or braces to transmit forces from not only beam end moments but also brace axial forces. In Taiwan, the fabrication of internal diaphragms for box columns typically employs fabrication details derived from Japanese steel-structure practices. In the past, the box column diaphragms were welded to column plates using electrogas welding (EGW). Today, welding is mainly performed by electroslag welding (ESW). The EGW or ESW is a single-pass vertical welding technique and commonly known as 'fishing welding'.

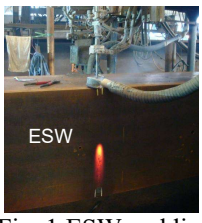

Fig. 1 ESW welding

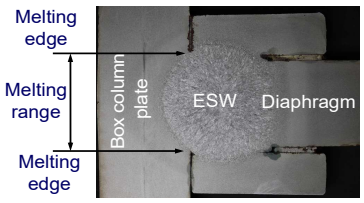

Fig. 2 Melting range of ESW

Previous research results on seismic steel beam-to-box column connections have shown that the strength of ESW welds at the T-shaped joint between the box column and diaphragm, which is subjected to beam flange force, may depend on the ESW melting range within the column plate (Fig. 2). In engineering practice, the ESW melting range on the column plate is determined by the two melting edges detected by vertical-probe ultrasonic testing (UT). In Japan, the ESW melting edges in column plates must meet the requirements of the "Standard for the Ultrasonic Inspection of Weld Defects in Steel Structures" published by the Architectural Institute of Japan (AIJ UIWD). In Taiwan, the requirements of CNS 12618 Annex A apply instead. However, the American Institute of Steel and Construction (AISC) lacks experience in applying ESW welding details on T-shaped joints between a diaphragm and a column plate within box columns. Furthermore, the American Welding Society (AWS) does not have an ultrasonic testing standard for detecting the melting range of ESW welds.

The various versions of AIJ UIWD (1989, 1996, 2008, and 2018) provide different vertical UT probe requirements for inspecting defects and for the melting range of the T-shape ESW joint connecting the diaphragm and box column plate. The different versions of AIJ UIWD specify different requirements for vertical UT probes as well. Table 1 lists the specifications of the vertical UT probes required by AIJ UIWD. According to the current CNS 12618 (2000), the specifications of the vertical UT probes to inspect defect and to detect melting range of the EWS welds are the same. Furthermore, both standards of AIJ UIWD (1996) and CNS 12618 (2000) adopt similar specifications for vertical UT probes, as shown in Table 1. It is clear from Table 1 that the probe specifications required by the current versions of both standards are different. This research investigates the probes used to detect melting range of ESW welds.

Table 1 Specifications of vertical UT probes for ESW weld quality and melting edge required by AIJ UIWD and CNS 12618 Annex A.

Version		Welds quality Probe (Diam./Freq.)	Welds edge Probe (Diam./Freq.)
AIJ	1989, 1996	ϕ20mm/5 MHz	ϕ20mm /2 MHz ϕ10 or 20mm /5 MHz
	2008, 2018	t ≤ 16mm ϕ10mm /5 MHz 16< t ≤ 60mm ϕ20mm /5 MHz 60mm< t ϕ28 or 30mm/2 MHz	ϕ10mm/5 MHz
CNS 12618 Annex A (2000)		ϕ20~25mm/4~5 MHz	ϕ20~25mm/4~5MHz

A series of vertical UT inspections for the melting edge for melting range of ESW welds on column plate surfaces was conducted using five probes. Two of the probes had a 10 mm diameter, which met AIJ UIWD requirements, using oscillation frequencies of 2 and 4 MHz. The other three probes had a 24 mm diameter, which met CNS 12618 requirements, using oscillation frequencies of 2, 4, and 5 MHz. Figure 3 shows the measurement results as a distribution of melting-edge percentage errors for the various probes. The results indicate that the two ϕ10 mm probes are more accurate than the ϕ24 mm probes. The ϕ10 mm probes display cumulative error percentages larger than 86% between ±2 mm. For the ϕ24 mm probes, the cumulative error percentage greater than 2 mm of absolute error is higher. In addition, it can be observed that the measurement accuracy increases with increasing oscillation frequency.

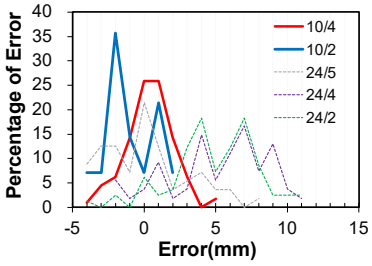

Fig. 3 Measurement error distribution for various probes

Based on the measurement results of the various probes, this article recommends replacing the ϕ20-25 mm/4-5 MHz vertical UT probe specified in CNS 12618 with the ϕ10 mm/5 MHz probe required in AIJ UIWD for inspecting the ESW melting range. (Ker-Chun Lin, kclin@ncree.narl.org.tw)

Seismic Rapid Evaluation Using AI Technology

Ying-Peng Wang, Project Assistant Technologist, NCREE
Tsung-Chih Chiou, Research Fellow, NCREE

Seismic Rapid Evaluation can swiftly screen the seismic resistance of at-risk buildings . Traditional seismic rapid evaluation relied on laborious manual processes, proving time and resource-intensive, to extract crucial data from engineering blueprints, such as cross-sectional areas of structural components. Thus, this study devised a computer vision and deep learning-based method for extracting vital building component data. By merging this with existing seismic rapid evaluation techniques, the goal is to expedite evaluation and minimize errors.

This study's method begins with aligning architectural and structural drawings using affine transformation. Then, walls are automatically cropped and classified using computer vision and deep learning. Next, image processing techniques identify wall length and thickness, yielding key parameters for cross-sectional area calculation. Finally, by integrating column and wall data, seismic preliminary assessments are conducted using established methods. The method has been tested on 181 buildings, achieving a 90.6% accuracy rate and a 96.1% confidence level and is thus suitable for engineering applications.

Methodology Development and Implementation

Figure 1 illustrates the method flowchart with inputs of architectural drawings and structural drawings. The ground floor drawings of the buildings are employed. Initially, image alignment is performed using affine transformation based on the least squares method. Simultaneously, pixel unit conversion is conducted on the architectural drawings to establish the pixel-to-centimeter ratio, calculated by sampling values in the X and Y directions. In the structural drawings, column component positioning is executed to determine the quantity and positions of column components. Users crop templates corresponding to each size to obtain the quantity and positions of column components through template matching. As a result, column cross-sectional area can be calculated. Subsequently, based on the resulting column component positions and image alignment data, wall component positioning is carried out to crop wall components from the architectural drawings. Since effective walls must align within frame lines, the program crops the wall images according to the frame line regions.

After cropping the images, wall component classification is performed to categorize whether the frame line images represent effective walls, namely four-sided confined walls or three-sided confined walls. For this purpose, a neural network-based classification model with an 86.6% accuracy rate was developed. Users further determine whether the images of effective walls represent reinforced concrete (RC) walls or brick walls. Following wall component classification, wall cross-sectional area calculation is conducted to calculate the cross-sectional area of effective walls. For this, a computer vision-based method was developed, involving vertical and horizontal projections of images to obtain the thickness and length of cross-sections. Additionally, since wall component thicknesses are regulated in the field of architecture, a set of criteria is applied to normalize the thicknesses.

Finally, using the basic parameters of the building along with the column cross-sectional result and wall cross-sectional result, the seismic index E value can be calculated.

Results

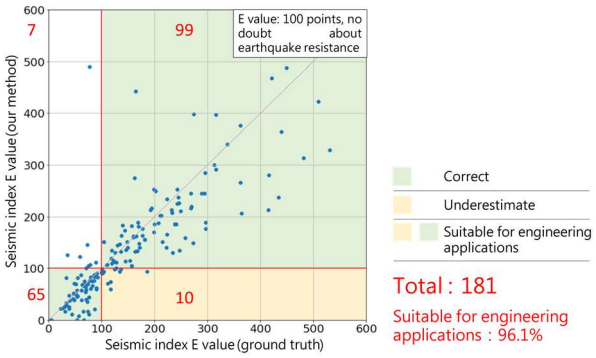

Fig.2. Validation results

The seismic index E value obtained by applying the method outlined here was verified by comparison with the manually calculated rapid evaluation index score (ground truth). Taking a seismic index E value greater than 100 (no doubt about earthquake resistance) as the grading benchmark, the verification results are shown in Figure 2. This method has already been applied to assess 181 buildings, with a 90% accuracy rate and a confidence level suitable for engineering applications of up to 96.1%.

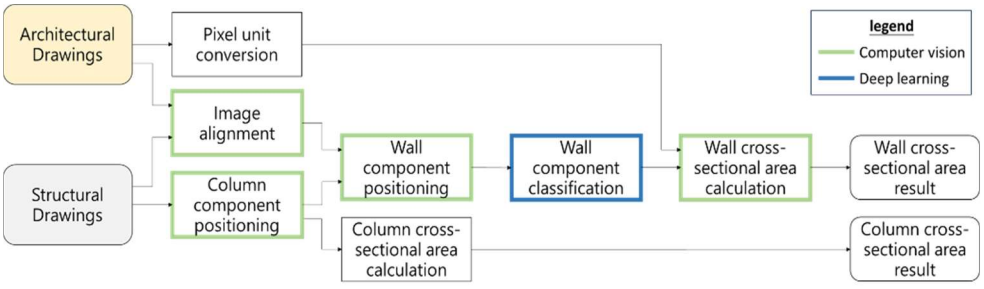

Fig. 1. Method flowchart

Seismic Evaluation of Steel Buildings (TEASPA-S)

Min-Lang Lin, Associate Researcher, NCREE
Te-Kuang Chow, Associate Technician, NCREE
Tsung-Chih Chiou, Researcher, NCREE
Lap-Loi Chung, Honorary Advisor, NCREE
Hui-Yu Chang, Research Assistant, NCREE

In Taiwan, detailed evaluations of the seismic capacities of reinforced-concrete building structures are very common, both in the study of assessment methods and in engineering practice. However, the gradual aging of buildings and continuous updates to design specifications may lead to the seismic capacities of existing steel structures in Taiwan becoming insufficient. In recent years, the number of new buildings using steel structures has increased, resulting in a greater need for earthquake-resistance assessment and reinforcement of steel structures.

The detailed evaluation method for the seismic capacity of a steel structure developed in this research is a continuation of the principles of that for a reinforced-concrete building developed by the National Center for Research on Earthquake Engineering's (NCREE) detailed evaluation method of the seismic capacity, called the Taiwan Earthquake Assessment for Structures by Pushover Analysis (TEASPA). The evaluation method is based on the Applied Technology Council's ATC-40 capacity spectrum method and nonlinear static pushover analysis. The evaluation method also uses the ETABS program, which is commonly used by local engineers to perform nonlinear static pushover analysis to obtain the capacity curve of a structure. The capacity curve is then converted into a seismic performance curve through the capacity spectrum method to evaluate the seismic performance of the structure.

This research has resulted in the publication of the second edition of the Seismic Evaluation Manual for Steel-Structure Buildings (TEASPA-S V2.0), which provides recommended parameters for component nonlinear hinges in welded box steel columns, H-shaped steel beams, and H-shaped concentric diagonal braces.

During the 1994 Northridge earthquake in the United States, many of the damaged steel structures primarily exhibited brittle failure of beam-column joints, and the plastic deformation angle of some beam-column joints was less than 0.015 rad. In 2000, the Federal Emergency Management Agency (FEMA 350) proposed a new form of certified joint (prequalified connections) to improve the ductility performance of beam-column joints. For this reason, the evaluation method developed by this research considers two joint types—traditional joints and improved joints— to determine recommended seismic performance criteria for each.

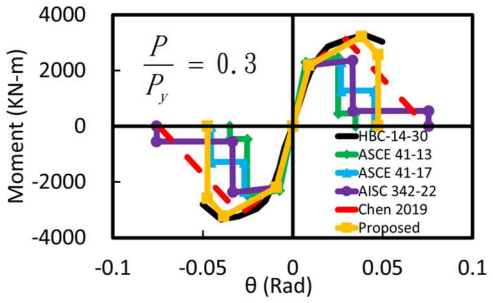

Fig. 1. Comparison of test envelope curves of box-shaped steel columns and the recommended nonlinear hinge curve

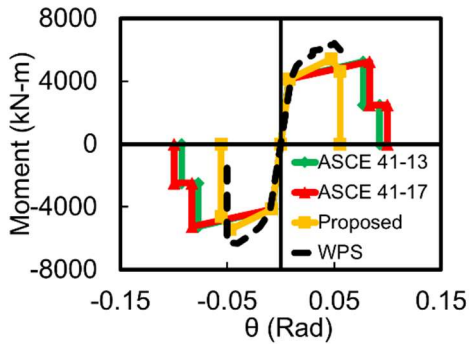

Fig. 2. Comparison of test envelope curves of H-shaped steel beams and the recommended nonlinear hinge curve

Figures 1 and 2 compare the nonlinear hinge curves of the box-type steel columns and H-shaped beams, respectively, with the experimental results from specimen responses. The nonlinear hinge curves recommended in this study can reasonably and conservatively respond to component behavior.

This study has already proposed eleven inspection items and methods that should be carried out during seismic assessment. The proposed techniques will assist engineers in ensuring the reasonableness of assessment results in order to avoid the misinterpretation of seismic assessment results and to maintain their accuracy.

Validation of the Numerical Model of the Extended NCREE Building Using Measured Seismic Responses

Ming-Chieh Chuang, Associate Researcher, NCREE

The project for the vertical addition to the National Center for Research on Earthquake Engineering (NCREE) building began in March of 2019. The extended NCREE building (Fig. 1) is a composite structure, consisting of an existing six-story reinforced concrete (RC) structure and an added seven-story steel structure. In addition, a new service core was added at the north side of the building from the first floor to the roof. To sustain the added steel structure, the existing RC structure was strengthened using added RC shear walls and fiber-reinforced polymer (FRP) strengthened RC beams. Moreover, buckling-restrained braces (BRBs), steel panel dampers (SPDs), and fluid viscous dampers (FVDs) were utilized in the added steel structure to improve the seismic performance.

In addition, the smart structural monitoring system (SSMS) was installed on the extended office building to act as the on-site earthquake early warning system as well as enabling long-term monitoring and investigation of its seismic response. Hence, the ambient and dynamic responses of the extended building can be monitored. Specifically, thirteen triaxial accelerometers (TAs) and thirty uniaxial accelerometers (UAs) were installed as the sensors for the instrumentation to monitor the floor responses. Figure 2 shows the layout of the accelerometers. A layout consisting of three uniaxial accelerometers was installed at positions A, B, and C identically across all stories except for the B1, 6th, 7th and 13th stories, where three to four triaxial accelerometers were installed instead. The accelerometers installed at positions A, B, and C were installed on the ceiling, while the accelerometers at position D were installed on the floor. When the SMSS is triggered by a seismic event, a 360-second stream of recorded data is retrieved from the data logger and entered on the Taiwan Structural Monitoring Data Hub (TSMOD, https://bas.ncree.org) developed by the NCREE.

To understand the seismic performance of the extended NCREE building, a collaborative research project was conducted by NCREE researchers and Prof. Keh-Chyuan Tsai's research group from the National Taiwan University. In the research, a variety of numerical models constructed using PISA3D structural analysis software were used to carry out a series of analyses including modal, pushover, and nonlinear response history analyses. The researchers utilized the measured structural responses of the earthquake from January 3, 2022, available on TSMOD, to examine the accuracy of the PISA3D model. Figure 3 compares the measured seismic responses and the simulation results of the PISA3D model with the full flexural and shear rigidities of beams, columns and walls, incorporating the presence of window sills and composite beam effects. The satisfactory simulation results imply that the stiffness and the mass distribution estimation are reasonable. Thus, the accuracy of the numerical model for predicting the small earthquake responses of the extended building remaining elastic is validated.

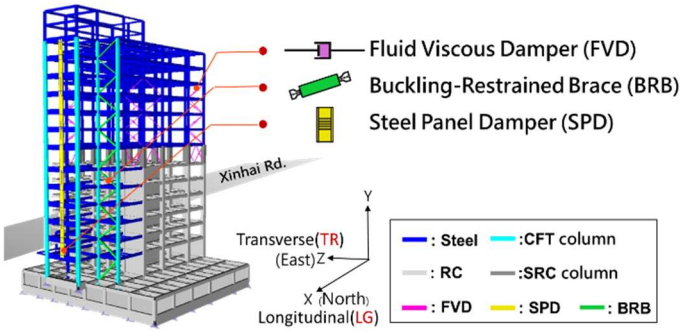

Fig. 1. PISA3D model of the extended NCREE building

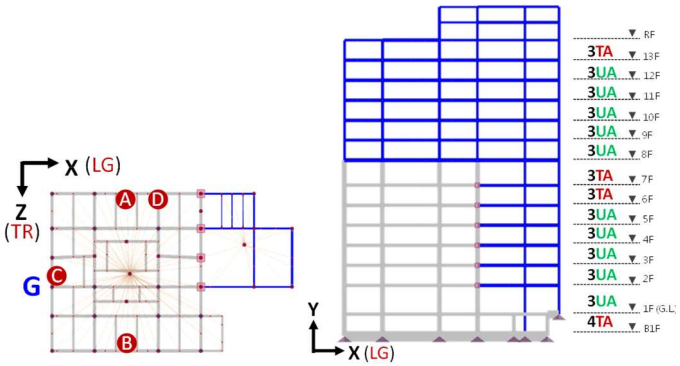

Floor Framing Plan Elevation (Line G)

Fig. 2. Instrumentation layout

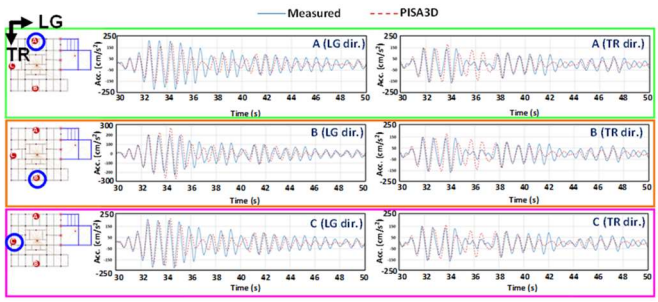

Fig. 3. Floor acceleration histories of the roof during the earthquake on January 3, 2022

Analysis of Truss-Confined Buckling-Restrained Braces

An-Chien Wu, Associate Researcher, NCREE

Development of TC-BRB

The key feature of the proposed truss-confined buckling-restrained brace (TC-BRB) is an additional truss confining system attached externally to the central steel casing (Fig. 1). The truss system is composed of several steel open-web truss frames and provides the required restraining rigidity, thereby reducing the central casing section size and the amount of infilled mortar. The hysteresis behavior of the TC-BRBs in terms of truss member response, buckling resisting ability, and cumulative deformation capacity was investigated through cyclic loading tests on physical specimens with different yield capacities, truss frame shapes, and sizes. The results confirmed that the proposed TC-BRB can be designed and fabricated to achieve excellent seismic performance.

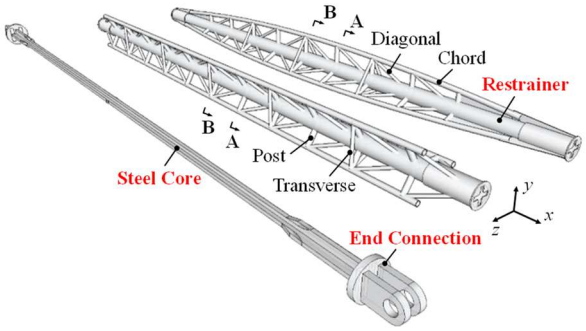

Fig. 1. Schematic of the TC-BRB

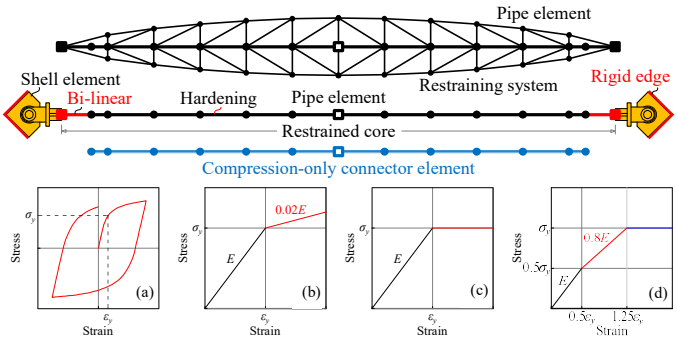

Fig. 2. Sketch of the proposed FEMs

Numerical Analysis of TC-BRB

A numerical procedure using finite element models (FEMs) is introduced to simulate the hysteresis responses of the specimens. The restrained steel core, central casing, and truss confining system were represented utilizing wire model with pipe element (Fig. 2). Meanwhile, the unrestrained steel core, end connections, and gusset plates were modeled using shell elements. The wire model for the restraining system was partitioned at the joints of each truss segment, and the restrained core was partitioned at corresponding positions of these divided points on the restrainer. To simulate the flexurally deformed core resisted by the restrainer, each pair of nodes on the restrained core and the central casing was coupled to exhibit identical translations in both transverse directions. Additional constraints were assigned to the pair of nodes at the midspan to ensure identical longitudinal translations and rotations. All degrees of freedom between the restrained core and end connection were coupled together. A separate axial connector element was parallel connected to each pair of nodes along the yielding portion to emulate compressive over-strength behavior. A hardening material was used for the pipe elements within the core yielding portion. A bi-linear material with a 2% post-yield stiffness was employed for all shell elements and two pipe elements at both ends of the restrained core. An elastic-perfectly plastic material was used to fabricate the pipe elements of the restraining system. A tri-linear material was used to fabricate the pipe elements of the chords.

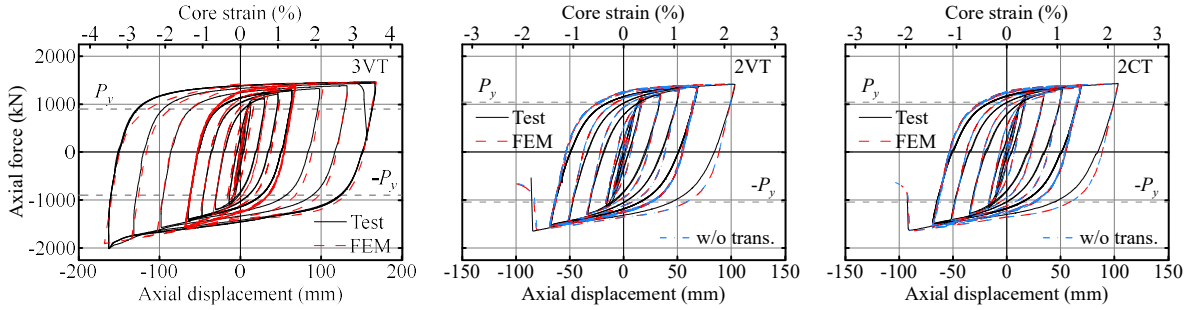

Fig. 3. Experimental and numerical responses of the specimens

The hysteresis responses depicted in Fig. 3 revealed that the overall agreement between the numerical and experimental results was remarkable. The proposed analytical procedures for calculating elastic buckling strengths and the numerical simulation method are deemed reliable. Moreover, the results confirmed that the contribution of transverse components to the overall buckling restraining mechanism was negligible. Numerical results indicated that the modeling method employed between the restrained core and the central casing can prevent numerical instability encountered when simulating the intricate hard contact and friction characteristics with solid elements. Additionally, the compression-only connector elements parallel-connected to the steel core prove efficient in reflecting realistic BRB compressive responses.

Nonlinear Dynamic Analysis for Seismic Retrofitting Applications

Pu-Wen Weng, Associate Researcher, NCREE
Chia-Chen Lin, Associate Technologist, NCREE
Fu-Pei Hsiao, Research Fellow, NCREE
Chih-Hsun Huang, Master student, NTUT

In the early morning of February 6, 2016, a severe earthquake struck the Meinong District of Kaohsiung City, Taiwan, leading to numerous mid-to-high-rise buildings collapsing and causing significant casualties. The primary reasons attributed to the collapse of these structures during the earthquake were poor structural system configuration, weak story conditions, and torsional effects. To effectively identify and mitigate these issues through structural numerical analysis, the National Center for Research on Earthquake Engineering proposed the "Taiwan Earthquake Assessment for RC Structures by Dynamic Analysis (TEASDA1.0)" (Hsiao et al., 2021), alongside an auxiliary program for conducting nonlinear dynamic analysis (Fig. 1). The objective was to adequately address concerns regarding the inadequate seismic performance of existing structures.

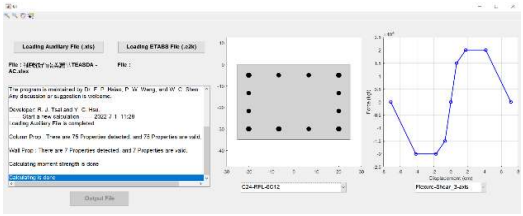

Fig. 1. Interface of the TEASDA auxiliary program

The seismic response of mid-to-high-rise buildings presents greater complexity and uncertainty compared with low-rise buildings. Conventional nonlinear static analysis for seismic assessment may fail to accurately predict the response of high-frequency mode shapes, potentially leading to non-conservative results. Consequently, this method is employed in conjunction with ETABS structural analysis software for comprehensive analysis.

The case study is a seven-story reinforced concrete residential building comprising one underground level. The eastern façade comprises shear walls with minimal fenestration. The ground floor accommodates commercial spaces and parking facilities. With irregular triangular dimensions measuring approximately 23.54 m in length and 19 m in width. To address weak story conditions and excessive torsional behavior, reinforced concrete (RC) frames were added around the perimeter of the ground floor. The numerical model of the retrofitted structure is depicted in Fig. 2.

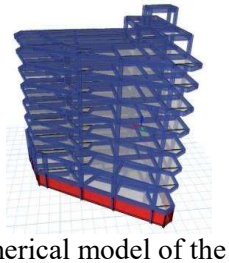

Fig. 2. Numerical model of the study case

In this study, a set of seven ground motion records was utilized. The "Platform of Input Motion Selection for Taiwan (INMOST)" was employed to select input earthquakes (Liu et al., 2020), ensuring compliance with seismic design codes (Ministry of the Interior, 2021) during dynamic time history analysis. The platform automatically selects suitable ground motion records from the database, ensuring that spectral acceleration values within the range 0.2T1 to 1.5T1 do not fall below 90% of the design spectral acceleration value, and the average value within this range meets the design spectral acceleration value. Finally, seven time history records best fitting the design response spectrum were selected for dynamic analysis.

By averaging the maximum inter-story drifts for each floor from the seven ground motions, the average inter-story drifts for each floor were determined. Comparison of before and after retrofitting linear plots of the average inter-story drifts in the X direction (Fig. 3) reveals that seismic retrofitting with additional RC outriggers around the ground floor effectively enhances the seismic performance of lower floors. However, for floors above the third floor, where no retrofitting was implemented, inter-story drifts still exceed displacement limits defined by an occupancy coefficient of I = 1.0 (2.5%), failing to meet performance standards.

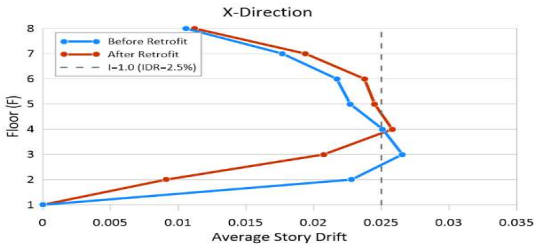

Fig. 3. Average inter-story drifts before and after retrofitting in the X direction

References

1. Hsiao, F-P., Tsai, R-J., Weng P-W., Shen W-C., Hsu, Y-C., Chow, T-K., Weng Y-T., Jean W-Y., Lin, C-C., Liu H-J., (2021). “Taiwan Earthquake Assessment for RC Structures by Dynamic Analysis (TEASDA 1.0), ” National Center for Research on Earthquake Engineering Technical Report, NCREE-21-001.
2. Liu, H-J., Lu, X-M., and Jean W-Y., (2022). “Platform of Input Motion Selection for Taiwan (INMOST),” 2021 NCREE Research Programs and Accomplishments, pp. 173-176.
3. Ministry of the Interior, Construction and Planning Agency, Taiwan (2021). “Building Seismic Design Code and Commentary.”

Seismic Study on Shear-type Seismic Stud Columns

Sheng-Jhih Jhuang and Kai-Ning Chi, Assistant Researcher, NCREE
Ker-Chun Lin, Research Fellow, NCREE

Previous studies have demonstrated that the core section of the web can stabilize energy dissipation behavior when shear-yielding stud columns without axial force are equipped with appropriate stiffeners and when appropriate attention is paid to welding details. For seismic stud columns (SSCs) with relatively short shear energy dissipating segments, the design requirements in moment-resisting frames can be easily satisfied. However, plastic shear behavior is influenced by relatively small relative interstory deformation. In the present study, four full-scale shear-type SSC specimens, each with a height of 2.5 m, were designed, and cyclic load tests were conducted using a multi-axial testing system (MATS) in the large structural laboratory at the National Center for Research on Earthquake Engineering. The objective of this study was to develop an SSC that maintains elasticity within the statutory limit of an interstory drift angle of 0.005 rad and while experiencing plastic deformation beyond this limit. This study provides suggestions for the design and construction of SSCs with both strength and energy dissipation performance.

The dimensions of the SSC specimens are indicated in Figure 1. All specimens had a height of 2.5 m, resembling SSCs in a building with a height of 3.3 m and a beam depth of 0.8 m. The specimens were constructed using H-shaped steel with a grade of A572 Gr.50 and with a yield strength of 345 MPa. During specimen preparation, the web plate corresponding to the height of the core segment in the center of the H-shaped steel was removed. Subsequently, top and bottom stiffeners were welded, followed by the embedding of A36 steel plates with a yield strength of 250 MPa in the stiffeners. Stiffeners were welded on both sides of the A36 steel plate in accordance with research parameters including the web width-thickness ratio (b/t) of the core segment and the arrangement direction of stiffeners (parallel or perpendicular to the shear direction). The top and bottom stiffeners and the core segment web stiffeners were composed of A572 Gr.50 steel plates. The four specimens in this study were labeled B1C06D20, B1C06D60, B2C10D35, and B2C12D35 based on the primary research parameters. The first two characters, B1 and B2, represent H-shaped steel sections, namely H588×300×12×20 and H608x306x18x30, respectively, used for producing the SSC specimens. The three characters beginning with C in the middle indicate the web thickness of the core segment, with C06, C10, and C12 representing thicknesses of 6 mm, 10 mm, and 12 mm, respectively. Finally, the last two letters starting with D indicate the ratio δ of the height of the core segment to the overall net height of the SSC, expressed as a percentage. All tests were conducted on the MATS system. The height of the specimen, including the top and bottom fixtures, was 3,500 mm. The top and bottom ends of the SSC specimen were fixed to the reaction frame and loading platform of the MATS system, respectively, using an appropriate number of prestressed steel rods. Two 1,200 kN vertical actuators were positioned on the south and north sides of the specimen, respectively. Two hydraulic servo actuators were arranged horizontally to apply a shear force to the specimens. One end of the actuator was connected to the loading platform, while the other end was secured on the reaction wall. The actuator was controlled using the MATS control system, and all tests were executed by applying the interstory drift loading of the American Institute of Steel Construction (AISC) 341-16 sequence for beam-to-column moment connections to the loading platform at the bottom of the fixed specimen. Throughout the tests, the vertical axial force on the specimens remained at zero.

The hysteresis loops depicting deformation and strength for the four specimens are shown in Figures 2 and 3. The test results indicated that the failure modes of all four specimens occurred subsequent to the generation of a tension field on the core segment web. The core segment web underwent concave folding and fracturing under the action of repeated tension and compression buckling, with ruptures occurring at the web center and edge welding joints of the web panel. The results of the strength tests on each specimen indicated that the yield shear strength of the core segment web could be precisely estimated using $V_y = 0.48F_yt_{wd}$. Additionally, the shear strain hardening factors of the core segment web were determined by dividing the maximum shear strength by the actual plastic shear strength of the specimen, and the factors for the four specimens were 1.61, 1.30, 1.62, and 1.41. Comparison of the shear strain hardening factors with the tension field angle (the angle with the horizontal axis) revealed that a larger tension field angle corresponded to a smaller strain hardening factor. The test results of the four specimens also indicated that the shear plastic deformation behavior of the core segment web was primarily influenced by the width-thickness ratio of the short side of the panel formed by the stiffeners and the flanges. In addition to the test results, data from six shear-type SSC specimens were collected from the literature so that data were available for ten test specimens. Linear regression analysis revealed a nearly linear relationship between shear deformation capacity (γ) and the short-side width-thickness ratio (b/t) of the core segment web before the tension field developed. The relationship between the two parameters can be expressed as $\gamma = -0.46(b/t) + 24.2$, indicating that a smaller width-thickness ratio of the short side of the core segment web results in a larger shear deformation capacity. Based on this relationship, the core segment stiffeners for shear-type SSCs can be accurately designed to achieve an effective shear deformation capacity.

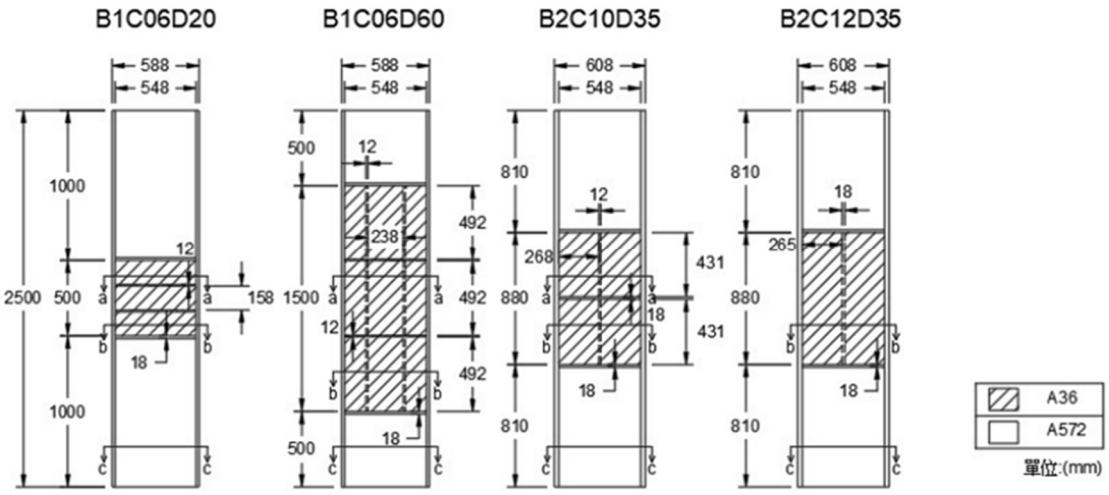

Fig. 1. Diagrams of the SSC specimens

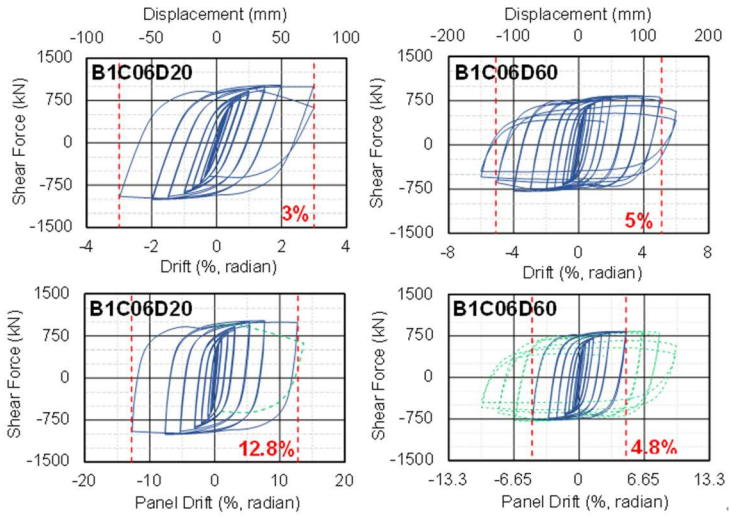

Fig. 2. Hysteresis loops of deformation and strength for specimens B1C06D20 and B1C06D60

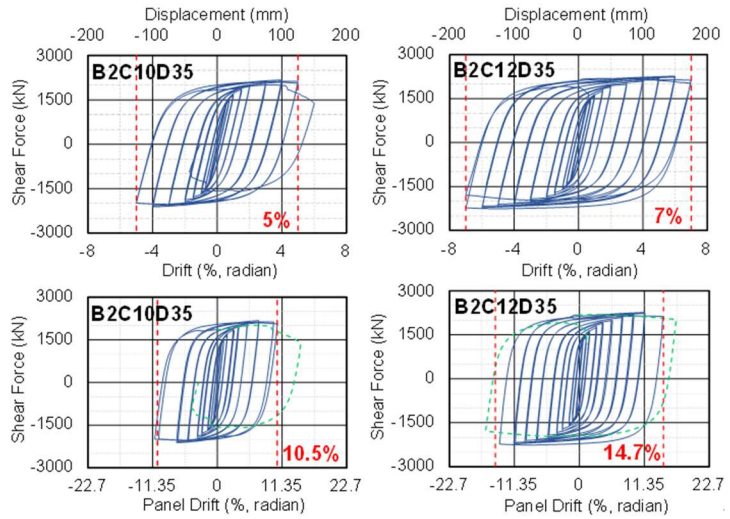

Fig. 3. Hysteresis loops of deformation and strength for specimens B2C10D35 and B2C12D35

Confinement Reinforcement of High-Strength Reinforced Concrete Tied Columns under High Axial Loads

Wen-Cheng Shen, Assistant Researcher, NCREE
Shyh-Jiann Hwang, Professor, NTU

Due to the scarcity of land, buildings are tending toward high-rise development. The ground story columns of high-rise buildings carry the weight of the entire building. Hence, they are under high axial load. At the same time, they must resist the repeated lateral movements caused by earthquakes. The use of high-strength materials can reduce the sectional size of the ground story columns and hence increase the residential space. Moreover, energy consumption and carbon emission can be significantly reduced by using high-strength reinforcing bars and concrete.

As the compressive failure behavior of high strength concrete (HSC) is brittle, the deformation ability of the structural member may be affected. Therefore, the ACI 318-19 building code requires that columns using HSC (f'c > 70 MPa) must increase the amount of confinement reinforcement to ensure sufficient confinement effectiveness and the development of ductile behavior. If the applied axial load on the column is higher, the deformation capacity will be correspondingly reduced. The ACI 318-19 building code further requires that when the applied axial load ratio exceeds 0.3, each longitudinal rebar around the column core should be engaged by transverse reinforcement with seismic hooks to provide lateral support. This requirement is easy to achieve if pre-assembled reinforcement cages are used. However, reinforcement cages in many parts of the world are mainly assembled on site. Schematic diagrams of test specimens are shown in Fig. 1.

The comparison of backbone curves are plotted in Fig. 2. The key findings are summarized as follows:

(1) The amount of confinement reinforcement of the column must be adjusted as the axial load changes. When the column bears higher axial load, more confinement reinforcement should be configured to maintain sufficient deformation capacity.

(2) Specimens T70-1 and T70-N42-D4 that comply with the confinement requirements of the ACI 318-19 building code exhibited an ultimate drift ratio greater than 3% in the positive and negative directions.

(3) The deformation capacities of the two specimens that had full laterally supported longitudinal reinforcement (Specimens T70-1 and T70-N42-D4) were better than the specimen that had partial laterally supported longitudinal reinforcement (Specimen B4).

(4) Specimen T70-2 with a 180-degree seismic hook at one end and a 90-degree hook at the other end in a staggered configuration does not conform to the requirements of the ACI 318-19 building code for a column subjected to high axial load, but it yielded no significant difference compared with Specimen T70-1, which had 180-degree hooks on both ends. A deformation capacity greater than 3% was still achieved for specimen T70-2. The test results show that the configuration of Specimen T70-2 should be feasible, and it may be possible to consider loosening the requirements of the ACI 318-19 building code with seismic hooks on both ends. However, further work is needed to explore this matter.

(5) The seismic behavior of Specimen T70-2 with a 180-degree seismic hook at one end was better than that of Specimen T70-N46-D3 with a 135-degree seismic hook at one end.

(6) Specimens T70-1 and T70-N42-D4 using crossties with 180-degree seismic hooks at both ends achieved the expected seismic performance. Moreover, construction of such a configuration on-site is easier than construction using 135-degree seismic hooks due to difficulties arising from the close arranged of elements that is required.

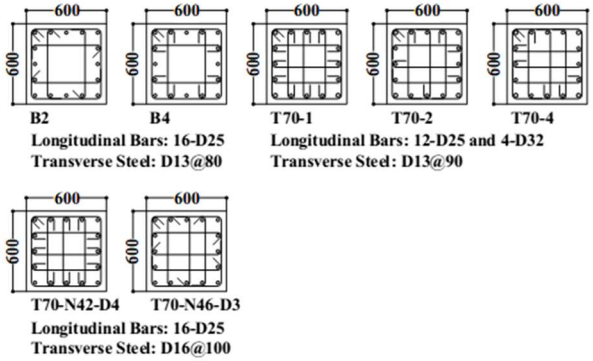

Fig. 1. Cross section of column specimens

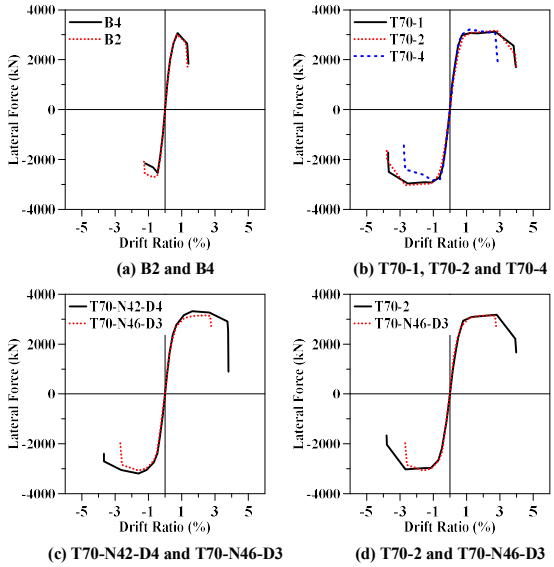

Fig. 2 Comparison of backbone curves

Soft Retrofit - An Interior Seismic Retrofitting Technique for RC Buildings Using Steel Elements

Te-Kuang Chow, Associate Technologist, NCREE
Yi-Hsuan Tu, Professor, NCKU
Tsung-Chih Chiou, Research Fellow, NCREE
Yuan-Tao Weng, Associate Researcher, NCREE

Street houses are the most common buildings in central and southern Taiwan. These structures are mostly made of reinforced concrete (RC) or reinforced bricks and they typically have similar floor plans. The characteristics of the structural system include a large number of partition walls perpendicular to the street, with ventilation, lighting, and circulation arrangements parallel to the street. However, under construction constraints, complete walls cannot be configured, resulting in insufficient earthquake resistance. In earthquakes, weak ground floor damage along the street direction occurs frequently, and existing low-rise RC buildings exhibit typical strong beam and weak column behavior. In the current implementation of seismic reinforcement of buildings in Taiwan, the reinforcement ratio in public buildings is considerably higher than that in private buildings. This is primarily because the public's awareness regarding disaster prevention is insufficient, and the cost of reinforcement and the obstruction of usability due to construction reduce the willingness of owners. Because of the restrictions on the plane type, commonly used reinforcement construction methods include adding RC shear walls, RC wing walls, steel diagonal bracing frames, expanded columns, or steel sheet cladding, etc. These are all difficult to implement because they affect the usability of the space or the bottom columns are close to the boundary. Professor Tu Yi-Hsuan of the Department of Architecture at National Cheng Kung University comprehensively considered the structural characteristics of typical street houses as well as user needs and proposed a set of simple reinforcement construction methods. Unlike the "hard reinforcement" that takes structural efficiency as the primary consideration, this "soft reinforcement" is a strong construction method expected to increase the willingness of private building owners to use seismic reinforcement with its characteristics of low cost, short construction period, and sufficient efficiency.

The Office of Retrofitting in Stages for Private Buildings of the NCREE endeavors to provide the engineering industry with a rapid reinforcement method for street houses. Professor Tu Yi-Hsuan has consented to share this reinforcement method, as well as its development background, mechanical theoretical model, single-column tests, frame tests, and comparative analyses with side thrust analysis, confirming that it can effectively provide reinforcement. Reference construction drawings were also drawn for use by technicians engaged in seismic reinforcement and repair.

The elevation of the pressure-bearing joint reinforced frame and the corresponding analytical model are introduced based on the previous test results, facilitating engineers in applying this reinforcement construction method for detailed assessments of actual building reinforcements, and to discuss the use of this method in typical street house cases. To improve the seismic performance of the reinforcement method, a structural analysis model was established using ETABS software. The TEASPA module and technical specifications for the design of steel structures for steel structures were used to calculate the nonlinear plastic hinges of the reinforcement components. Comparative analysis and test results were performed to verify the accuracy of the model.

Based on the results of component and frame tests, and using the experimental results as adjustment confirmation data, two expedient estimation methods are proposed, namely the simple estimation method A (individual section) and the simple estimation method B (composite section). Both estimation methods enable rapid lateral force strength analysis of the reinforced rear column to estimate the number of reinforced steel frames required. This can be used by designers to initially determine the number of required steel frames and serve as a subsequent structural model for detailed evaluation of side thrust with TEASPA.

In conclusion, the reinforcement design strategy of the "soft reinforcement" construction method, its advantages, disadvantages, and limitations, as well as precautions for review and implementation, are provided.

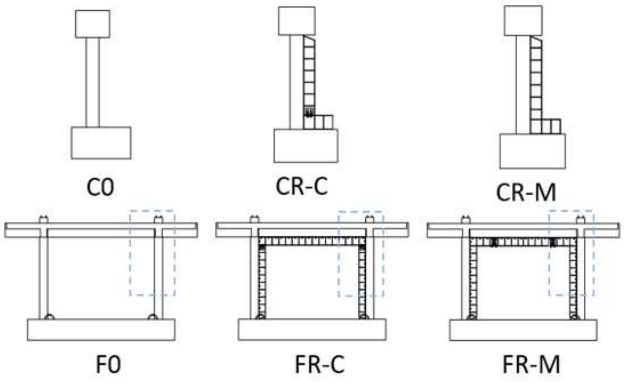

Fig. 1. Single column specimen
Frame specimen figure

Robotic Welding Technology for Continuity Plate Welding Within Steel Built-up Box Columns

Chung-Che Chou, Director General, NCREE
Gee-Jin Yu, Associate Technologist, NCREE
Chun-Yao Yang, Research Assistant, NCREE
Kung-Juin Wang, Principal Engineer, NCREE
Wei-Tze Chang, Associate Researcher, NCREE
Chiun-Lin Wu, Deputy Director General, NCREE

The demand for steel construction in Taiwan has increased rapidly in recent years. However, the steel fabrication industry is experiencing a shortage of qualified welders, which has already significantly impacted industry growth. Unfortunately, robotic welding has not yet been applied to building construction in Taiwan. The drive to reduce manufacturing costs has led to larger manufacturing discrepancies or geometric errors during plate cutting and unit assembly. Therefore, developing advanced robotic welding technologies has emerged as a critical solution for automating building construction in Taiwan.

The use of built-up box columns is a popular choice for steel buildings in Taiwan. To ensure adequate moment resistance at the beam-to-column connections, two continuity plates inside the box columns are welded to the beam flanges at each floor level. The weld quality of these continuity plates significantly influences the effectiveness of moment transfer from the beams to the columns, which, in turn, has a major impact on the overall seismic performance of steel frames during seismic events. Skilled welders remain indispensable for gas metal arc welding (GMAW), which is used in joining the continuity plates and column flanges.

This study, in partnership with four major domestic steel construction factories (Evergreen Steel Corporation, Chun Yuan Steel Industry Company, Tung Kang Steel Structure Corporation, and China Steel Structure Company), aims to develop an integrated GMAW system to automatically weld internal continuity plates to steel built-up box columns for the construction industry. The robotic welding system performs automatic welding work by measuring the profile of the current weld bead and setting the welding machine parameters using artificial intelligence.

The integrated robotic GMAW system in this study is divided into two subsystems: the robotic welding equipment and the welding monitoring equipment. In conventional welding procedures, welders manually control their welding apparatus. Conversely, within an integrated robotic GMAW system, the manipulator replaces the welder's hand, and the welding monitoring equipment replaces the welder's senses.

The robotic welding equipment includes a robotic manipulator, a welding machine, a water-cooled welding gun, an oxide removal device, and a wire feeder, among other components (Fig. 1). The welding method is consistent with the existing weld procedure for GMAW with CO2 as the shielding gas. Each piece of welding equipment needs to be is modified to accept welding instructions, which let the equipment could be integrated into a control system.

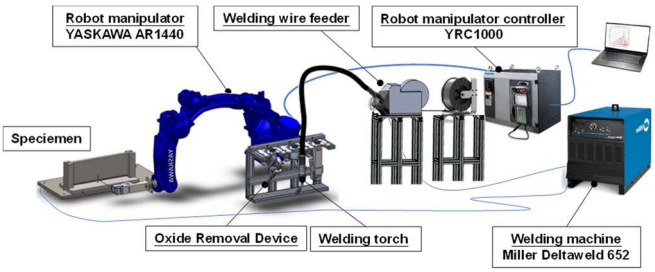

Fig. 1 Robotic GMAW equipment

Figure 2 shows the fabrication process of the specimens used in this study. The specimens were designed to emulate the connection details of a continuity plate, column flange, and beam flange in a typical steel box column. Figure 2(a) illustrates the initial assembly, where the continuity plate (marked in yellow) is placed in a position relative to the column flange (marked in orange) inside a built-up box column. As shown in Fig. 2(b), the specimen is composed of the continuity plate. Once all plates are positioned, a manipulator performs GMAW using different trial parameters to join the continuity and column plates, as shown in Fig. 2(c). The welding quality is then assessed by non-destructive testing (NDT), including visual testing (VT) and ultrasonic testing (UT). If the welding quality meets the AWS D1.1 standard, another steel plate representing the beam flange is manually welded using flux-cored arc welding (FCAW) to the opposite side of the column plate. This simulates the current construction practice in Taiwan, as shown in Fig. 2(d). The specimens were formed from SN490 steel plates. Finally, steel coupons are created by cutting and grinding the specimens for subsequent material testing.

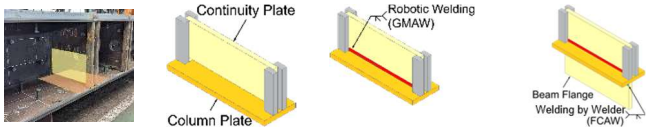

(a) (b) (c) (d)

Fig. 2 The specimen manufacturing process

This study aimed to develop an automated welding procedure to achieve multi-layer, multi-pass CJP welding between a continuity plate and a column flange plate. The effects of various manipulator control and welding machine parameters on dozens of specimens were examined. This, in turn, was used to develop an algorithm for automatically selecting welding parameters to perform automated welding.

Workshop of Needs and Aspirations for Disaster Prevention and Rescue Needs with Artificial Intelligence Technology

Jye-Hwang Lo, Assistant Researcher, NCREE
Wei-Tze Chang, Associate Researcher, NCREE
Cheng-Tao Yang, Associate Researcher, NCREE

In light of the increasing frequency of natural disasters and global challenges, the role of technology in disaster prevention, rescue, and humanitarian aid is becoming increasingly important. The NCREE-NTUCE Joint Artificial Intelligence Research Center (hereafter referred to as the AI Center) held the "Workshop of Needs and Aspirations for Disaster Prevention and Rescue Needs with Artificial Intelligence Technology" on December 27th, 2023, at the National Center for Research on Earthquake Engineering (NCREE). This workshop embarked on an exploration of deep learning methodologies integrating Artificial Intelligence (AI) with disaster prevention and rescue technologies. The primary objective of the workshop was to promote and leverage the application potential of innovative technologies, align research and development teams with disaster prevention and rescue needs, and explore how AI can play a crucial role during disasters.

Director Chuin-Shan Chen and four deputy directors of the AI Center, namely Chia-Ming Chang, Szu-Yun Lin, Je-Chian Lin, and Rih-Teng Wu, alongside Dr. Chin-Hsun Yeh, Dr. Tsung-Chih Chiou, and Dr. Cheng-Tao Yang from NCREE, led various research teams in presenting scenario designs and technological progress in addressing disaster-related challenges. The topics discussed included multi-dimensional earthquake disaster prevention and response platforms, the applications of Large Language Models (LLMs) in disaster prevention, recognition of large-scale disaster damage, three-dimensional modeling of disaster scenes and recognition, and post-disaster emergency assessment. Several invited units, such as the National Fire Agency of the Ministry of the Interior, the Fire Department and Secretariat of the Taipei City Government, the Taipei Water Department, the Fire Department of the New Taipei City Government, the Hualien County Government, and the Buddhist Compassion Relief Tzu Chi Foundation, provided insights into the current practical situation of central government agencies, local government bureaus, and civil organizations. They proposed various disaster prevention and rescue challenges they encounter.

Finally, a comprehensive discussion was held to discuss the directions of cooperation and planning between the AI Center, the NCREE, and various units, laying the groundwork for the future integration of AI technology across official, private, and civil sectors. The workshop successfully sparked inspiration among participants, fostering an environment where research and development teams and disaster prevention and rescue units could mutually stimulate ideas and exchange views, collectively exploring the potential of AI-assisted disaster prevention and rescue transformation, encouraging more innovation in disaster prevention and rescue initiatives, and striving to build a safer and more intelligent society. Participants are also set on witnessing the tangible outcomes of the various issues and applications discussed in the workshop and are hopeful that this will contribute to remarkable advancements in disaster prevention and rescue efforts.

Fig. 1. Welcome speech by Dr. Chuin-Shan Chen, director of the NCREE-NTUCE Joint AI Research Center

Fig. 2. Overview and needs sharing session regarding disaster prevention and rescue with AI technology

Fig. 3. Group discussion session

Fig. 4. Group photo featuring participants

NCREE Exhibits at CES 2024 and Signs MOU with ActiBooty Inc.

Ren-Zuo Wang, Research Fellow, NCREE
Chih-Shian Chen and Jui-Mien Lin, Assistant Researcher, NCREE

The Taiwan Tech Arena (TTA) of the National Science and Technology Council led a Taiwanese innovation team to participate in the International Consumer Electronics Show (CES) in the United States in 2024. This year's exhibition focused on six major areas: artificial intelligence and robotics, digital health, smart home, smart cities and sustainability, sport technology, and vehicle technology and advanced mobility. The exhibition showcased Taiwan's innovative technological advancements to the international community.

The Smart City Team of the National Center for Research on Earthquake Engineering (NCREE) was selected by the National Applied Research Laboratories (NARLabs) to showcase the "5D Smart Factory Platform", a practical application of 5D smart digital space. The project site is located in Thailand. This disaster prevention platform was introduced to reduce the impact of flooding caused by extreme weather in Thailand's coastal industrial areas. It also strengthens the monitoring of labor safety and environment in the factory. It is expected to use information integration to establish a 5D smart disaster prevention platform, fostering multilateral cooperation, facilitating technological exchanges, and increasing the competitiveness of the factory.

In addition, five "TTA Demo Show" events were conducted on the main stage of the TTA Pavilion this year, inviting international partners from South Korea, Japan, the Netherlands, Luxembourg, and France to participate in the event and showcase their latest technologies. The "5D Smart Factory Platform" was also selected for technical exchange at venues in South Korea and actively participated in activities organized by Business France.

Considering the widespread response received by the exhibition platform, a memorandum of understanding (MOU) was signed by Deputy Director General Chai Juin-Fu, representing the NCREE at CES 2024, with ActiBooty Inc., a South Korean 3D GIS platform developer, in the presence of the TTA of Taiwan, Jeonbuk Center for Creative Economy and Innovation of South Korea, and Operation & Promotion Office Director Chang Lung-Yao of NARLabs. To facilitate cooperation and exchange between the NCREE and South Korea in the field of science and technology, the NCREE will collaborate on the application of 5D smart platforms in smart cities based on mutual research and development efforts.

Fig. 1. Group photograph of the CES 2024 opening ceremony

Fig. 2. Group photograph featuring the NCREE team with Ms. Shirley Hsiu-Ya Yang, Director of the Science and Technology Division Taipei Economic and Cultural Representative Office in the U.S.

Fig. 3. Deputy Director General Chai Juin-Fu of NCREE signing the MOU with ActiBooty Inc. from South Korea

NCREE Signs MOU with the Earthquake Research Center of Thailand (EARTH)

Chia-Chen Lin, Associate Technologist, NCREE
Pu-Wen Weng, Associate Researcher, NCREE
Fu-Pei Hsiao, Research Fellow, NCREE

In 2014, a strong earthquake with a magnitude of 6.3 occurred in Chiang Rai Province in northern Thailand. This was the largest earthquake in a century in Thailand. Although it did not cause many casualties, it drew widespread attention to earthquake disasters across Thailand. Based on the continuous efforts of the Thai academic community in earthquake engineering research, the Thai government established the Earthquake Research Center of Thailand (EARTH) in 2023 to lead the Thai academic community in research on earthquake engineering.

The National Center for Research on Earthquake Engineering (NCREE) has executed the National Science and Technology Council's project, which actively promotes and exchanges technologies and experiences related to seismic assessment and retrofitting in the southbound region. In accordance with this project, the NCREE has been collaborating with the Asian Institute of Technology in Thailand and King Mongkut's University of Technology Thonburi to jointly promote seismic assessment and retrofitting of school buildings since 2021. Relevant retrofitting demonstration cases have been established through which the NCREE has established a good communication channel with the Thai academic research community. In order to continue to exchange relevant earthquake engineering technologies with Thailand, the NCREE has prepared for the signing of a cooperative memorandum of understanding (MOU). Led by Prof. Pennung Warnitchai, Director of the EARTH, a delegation comprising Prof. Nakhorn Poovarodom, Prof. Sutat Leelataviwat, and Prof. Natt Leelawat visited the NCREE on January 9, 2024. After the signing of the MOU, both parties committed to joint research endeavors in earthquake engineering-related research in the future. The research topics include the following: (1) earthquake simulation experiments on large structures, (2) building structure health monitoring system, (3) building structure seismic assessment and repair, and (4) academic exchange seminars.

The EARTH is an important institution for earthquake engineering research in Thailand. The NCREE has long been committed to earthquake engineering and disaster prevention research. This cooperation agreement will facilitate the mutual exchange of advanced earthquake engineering and disaster prevention technologies and integrate the research and development efforts of both parties for mutual benefit.

Fig. 1. Director General Chou Chung-Che of NCREE (left) and Prof. Pennung Warnitchai, Director of EARTH (right) sign the MoU for cooperation

Fig. 2. A group photo of NCREE and EARTH members after the MOU signing ceremony

Memorandum of Understanding between SESTEC and NCREE

Tzu-Chieh Chien , Associate Technologist, NCREE

The Seismic Research and Test Center (SESTEC) of Pusan National University of Republic of Korea strives to improve seismic- and vibration-related technologies by researching the seismic performance of public infrastructure and ensuring the safety of critical structures subject to dynamic loads. As an accredited testing institution in the field of seismic and vibration technologies, SESTEC establishes systematic procedures for test methods, trains the next generation of researchers, and promotes the development of new structural systems and new technologies.

The center utilizes existing facilities including shaking tables to provide testing services to professors, researchers, students, and industry personnel. This, in turn, enhances the educational value of the center's facilities and leads to the development of more practical applications. In addition to furthering experimental research in the seismic and vibration fields, the center also cooperates with international organizations, promotes international exchanges to address Korea's technological deficiencies, and improves infrastructure safety in the event of an earthquake.

To promote bilateral cooperation in science and technology development and to further strengthen the relations between SESTEC and National Center for Research on Earthquake Engineering (NCREE), Director Lee Sang-Ho and other researchers including Kim Jae-Bong and Oh Sang-Hoon among others from SESTEC in Korea visited Taiwan at the invitation of NCREE. On January 22, 2024, NCREE and SESTEC successfully held a signing ceremony for a Memorandum of Understanding (MoU), with Director General Chou Chung-Che representing NCREE (Figs. 1 and 2). The MoU states that both parties will decide on the areas of collaboration and joint research topics in accordance with the principles of equality, reciprocity, and cooperation. Both parties agree to mutually select the specific topics for joint research and development projects in the following areas of science and technology: earthquake engineering, experimental technology, and seismic design for non-structural systems. On a best-effort basis, both parties agree to facilitate the exchange of scientific and technical personnel between the organizations, including their associated institutes, to implement the MoU.

On the following day, January 23, the Director and researchers from SESTEC visited NCREE's Tainan Laboratory (Fig. 3). A workshop was held on the same day to exchange information, share recent testing methods and results for non-structural elements such as suspended equipment from ceilings and busways, and liquid storage tanks. The potential for future cooperation was discussed, with the goal of creating more opportunities for joint seismic engineering research between Taiwan and Korea.

Fig. 1. Director General Chou Chung-Che of NCREE (left) and Director Lee Sang-Ho of SESTEC (right) sign the MoU for cooperation

Fig. 2. A group photo of NCREE and SESTEC members after the signing ceremony

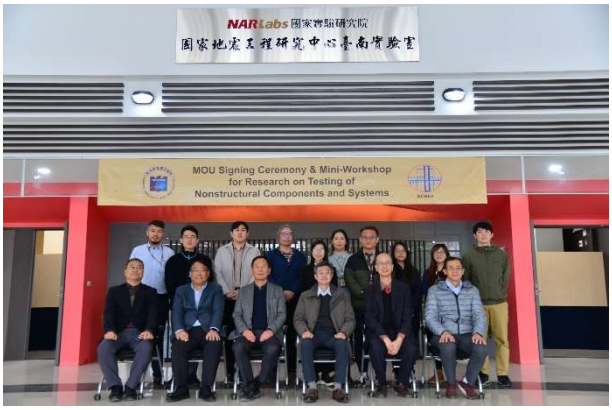

Fig. 3. A group photo of NCREE and SESTEC members at Tainan Laboratory